Electronic structure of spin-$\frac{1}{2}$ Heisenberg antiferromagnetic systems: $Ba_2Cu(PO_4)_2$ and $Sr_2Cu(PO_4)_2$

Sarita S. Salunke, M. A. H. Ahsan,* R. Nath,† A. V. Mahajan, and I. Dasgupta‡
Department of Physics, Indian Institute of Technology Bombay, Mumbai 400076, India
(Received 7 May 2007; revised manuscript received 27 June 2007; published 6 August 2007)

We have employed first principles calculations to study the electronic structure and magnetic properties of the low-dimensional phosphates, $Ba_2Cu(PO_4)_2$ and $Sr_2Cu(PO_4)_2$. Using the self-consistent tight-binding linearized muffin-tin orbital method and the *N*th order muffin-tin orbital method, we have calculated the various intrachain as well as the interchain hopping parameters between the magnetic ions (Cu^{2+}) for both the compounds. We find that the nearest-neighbor intrachain hopping (t) is the dominant interaction suggesting the compounds to be indeed one dimensional. Our analysis of the band dispersion, orbital projected band structures, and the hopping parameters confirms that the Cu^{2+}-Cu^{2+} super-super exchange interaction takes place along the crystallographic b direction mediated by O-P-O. We have also analyzed in detail the origin of short-range exchange interaction for these systems. Our *ab initio* estimate of the ratio of the exchange interaction of $Sr_2Cu(PO_4)_2$ to that of $Ba_2Cu(PO_4)_2$ compares excellently with available experimental results.

DOI: 10.1103/PhysRevB.76.085104 PACS number(s): 71.20.−b, 71.70.Gm, 75.10.Pq

I. INTRODUCTION

Low-dimensional quantum spin systems with chain, ladder, or planar geometries have attracted much attention due to their unconventional magnetic properties.[1] Much effort has been devoted particularly over the last decade to understand the behavior of quasi-one-dimensional spin systems. These systems exhibit a rich variety of phases due to the enhanced quantum fluctuations in reduced dimensionality. It is well known that the half-integer uniform antiferromagnetic chain, though having a singlet ground state, is gapless and quantum critical with power-law spin correlations. A deviation from the uniform chain due to, for instance, an alternating exchange leads to a gapped (spin gap Δ) ground state. Frustration arising in one-dimensional spin chains due to next-nearest-neighbor interactions can also lead to a gap in the spin excitation spectrum. A well known case is that of the Majumdar-Ghosh (MG) chain,[2] where the Hamiltonian is antiferromagnetic in nature and includes both nearest-neighbor J_1 and next-nearest-neighbor J_2 exchange interactions. This model is exactly solvable for the ratio $\frac{J_2}{J_1}=\alpha=0.5$. The MG chain supports a spin gap for $\alpha>\alpha_{cr}=0.2411$. For $0<\alpha<\alpha_{cr}$, a gapless phase is obtained. In contrast, integer-spin uniform antiferromagnetic chains are gapped as conjectured by Haldane,[3] as also half-integer even-leg ladders,[4] while the half-integer odd-leg ladders are gapless. Recently, the discovery of spin-Peierls transition in the one-dimensional (1D) Heisenberg antiferromagnet (HAF) $CuGeO_3$ (Ref. 5) renewed interest in 1D transition metal oxides with spin $S=\frac{1}{2}$ ions such as Cu, which are responsible for both the magnetic properties as well as the Jahn-Teller distortion of the lattice.

Low-dimensional quantum spin systems are important also due to the belief that understanding these systems may be crucial to understand the physics of high-T_c cuprates.[6] In addition, the field of low-dimensional quantum magnetism provides a fertile ground for rigorous theory. Powerful techniques such as the Bethe ansatz and bosonization are available to study ground and excited state properties of these systems. Models of interacting spin systems are known for which the ground state and, in some cases, their low-lying excitation spectra are known exactly. The knowledge gained from these models provides impetus to look for real materials so that experimental confirmation of the theoretical predictions can be made.

Quasi-1D magnets, in which the magnetic interaction in one direction dominates, with much weaker interactions in other directions, exhibit short-range order over a wide temperature range. A uniform Heisenberg half-integer-spin chain as discussed above has a gapless spin excitation spectrum. The ground state does not have long-range order (LRO) because of strong quantum fluctuations. In real systems, however, interchain interactions can lead to a deviation from ideal behavior and even magnetic LRO. Whereas a large number of quasi-1D systems have been studied, there are only a few cases in which the interchain interactions are very weak and true 1D behavior can be observed down to low temperatures. One example is Sr_2CuO_3 where the exchange coupling constant J/k_B is about 2200 ± 200 K and the ordering temperature $T_N=5.4$ K, giving the ratio $k_BT_N/J\approx0.25\%$.[7] Another example is copper benzoate, $Cu(C_6H_5COO)_2\cdot3H_2O$, with $J/k_B=17.2$ K.[8]

Very recently, the susceptibility measurements by Belik *et al.*[9] and susceptibility and nuclear magnetic resonance (NMR) measurements by Nath *et al.*[10] have suggested that $Ba_2Cu(PO_4)_2$ ($J/k_B=151$ K) and $Sr_2Cu(PO_4)_2$ ($J/k_B=165$ K) are excellent $S=\frac{1}{2}$ linear chain Heisenberg antiferromagnets. The temperature dependence of the NMR shift $K(T)$ is well described by the $S=\frac{1}{2}$ Heisenberg antiferromagnetic chain model.[11] The J/k_B in these compounds is about 1 order of magnitude smaller than in Sr_2CuO_3 and about 1 order of magnitude larger than in copper benzoate. In $Sr_2Cu(PO_4)_2$, Belik *et al.*[9] suggested from their measurements that LRO sets in at $T_N=0.085$ K, which implies that $k_BT_N/J=0.06\%$, making $Sr_2Cu(PO_4)_2$ the *best* realization of

a 1D $S=\frac{1}{2}$ HAF system studied to date. This provides a rare opportunity for a comparison of experimental results with theoretical models and improving our understanding on these systems.

The unique 1D magnetic behavior exhibited by these compounds may be traced back to the interplay of the geometry (crystal structure) and quantum chemistry and therefore requires a thorough understanding of the electronic structure of these systems. In this paper, we shall study the electronic structure of $Ba_2Cu(PO_4)_2$ and $Sr_2Cu(PO_4)_2$ in some detail. The characteristic feature of these compounds is a chain of isolated CuO_4 square plaquettes along the crystallographic *b* direction. The goal of the present work is to understand and evaluate the various exchange paths leading to 1D magnetism by calculating the various hopping integrals. The latter will also provide the dominant exchange integrals entering the magnetic Hamiltonian for the spin-half Heisenberg chain given by

$$H = -\sum_{ij} J_{ij}(\mathbf{S}_i \cdot \mathbf{S}_j), \tag{1}$$

where J_{ij} is the magnetic exchange interaction and *S* denotes the spin. The various hopping matrix elements between the magnetic ions (Cu for these compounds) are strongly dependent on the way the CuO_4 squares are assembled. The edge sharing CuO_4 squares and corner sharing CuO_4 squares lead to quite different values for the nearest-neighbor hopping (*t*) and the exchange interaction (*J*). In the latter case, the 180° Cu-O-Cu bond with a common O $2p$ orbital gives rise to large magnitude of *J* as seen for the CuO_2 planes in the high-T_c cuprates. This contrasts with the 90° Cu-O-Cu bond when two CuO_4 squares share an edge, where the hopping matrix element *t* and therefore the exchange interaction are expected to be small in magnitude. In the present work, we shall explicitly obtain the various effective Cu-Cu hopping parameters using the *N*th order muffin-tin orbital method (NMTO) and clarify the role of electronic structure on the magnetic properties of these systems.

The remainder of the paper is organized as follows: In Sec. II, we describe the crystal structure of both $Ba_2Cu(PO_4)_2$ and $Sr_2Cu(PO_4)_2$ followed by the computational details. Section III is devoted to the detailed discussion of the electronic structure using tight-binding linearized muffin-tin orbital method (TB-LMTO) within atomic sphere approximation (ASA) and the NMTO method followed by a comparative study of our calculations with available experimental results. Finally, in Sec. IV, we present our conclusions.

II. CRYSTAL STRUCTURE AND COMPUTATIONAL DETAILS

$Ba_2Cu(PO_4)_2$ and $Sr_2Cu(PO_4)_2$ are two isostructural compounds in the family of $S=\frac{1}{2}$ 1D HAF systems.[12] They both crystallize in the monoclinic structure with space group

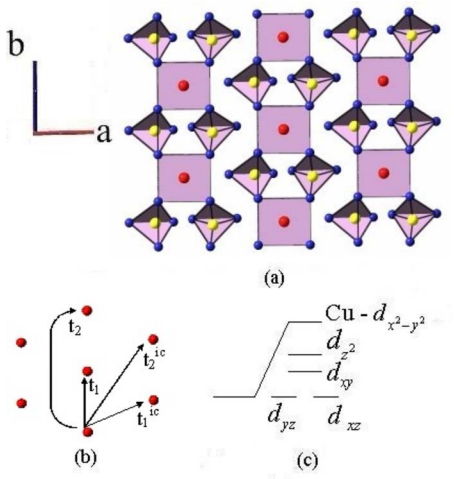

FIG. 1. (Color online) (a) Schematic diagram of $[Cu(PO_4)_2]_\infty$ linear chains propagating along the *b* direction for $(Ba/Sr)_2Cu(PO_4)_2$. (b) Various hoppings between the Cu atoms. (c) Schematic energy level diagram for a Cu *d* ion in square planar environment.

$C_{2/m}$ (No. 12). The lattice parameters are $a=12.16$ Å, $b=5.13$ Å, $c=6.88$ Å, and $\beta=105.42°$ and $a=11.51$ Å, $b=5.07$ Å, $c=6.57$ Å, and $\beta=106.35°$ for $Ba_2Cu(PO_4)_2$ and $Sr_2Cu(PO_4)_2$, respectively. The characteristic features of the structure as illustrated in Fig. 1 are isolated, square, CuO_4 plaquettes sharing their edges with two similar kinds of PO_4 tetrahedra. This edge sharing via PO_4 tetrahedra takes place along one crystallographic direction (*b* direction), forming isolated $[Cu(PO_4)_2]_\infty$ chains along the crystallographic *b* direction. The chains are, however, staggered with respect to each other along the crystallographic *a* direction. The Ba/Sr cations reside between these parallel chains. In Fig. 1(b), we have indicated the hoppings between various Cu atoms. In Fig. 1(c), we have displayed the schematic energy level diagram due to crystal field splitting of the Cu *d* ion in the square planar coordination provided by the oxygens. We find that the highest energy level is Cu $d_{x^2-y^2}$ and is well separated from the rest of the Cu *d* levels.

Our analysis of the electronic structure is carried out in the framework of the TB-LMTO method[13,14] in the ASA within local density approximation (LDA) to the density functional theory. The space filling in the ASA is achieved by inserting empty spheres and by inflating the atom-centered nonoverlapping spheres. The atomic radii are chosen in such a way that (i) the charge on the empty spheres is negligible and (ii) the overlap of the interstitial with the interstitial, atomic with the atomic, and interstitial with the atomic spheres remains within the permissible limit of the ASA. The basis set for the self-consistent electronic structure calculation for $Ba_2Cu(PO_4)_2$ includes Cu (*s*, *p*, *d*), Ba (*s*, *d* and *f*), O (*s*, *p*), and P (*s*, *p*), and for $Sr_2Cu(PO_4)_2$, the basis set includes Cu (*s*, *p*, *d*), Sr (*s*, *d*), O (*s*, *p*), and P (*s*, *p*), the rest being downfolded. The (8, 8, 8) *k* mesh has been used for self-consistency. All the *k*-space integrations were performed using the tetrahedron method.[15] In order to extract the various hopping integrals, we have employed NMTO based downfolding method.[16–18] The downfolding method consists

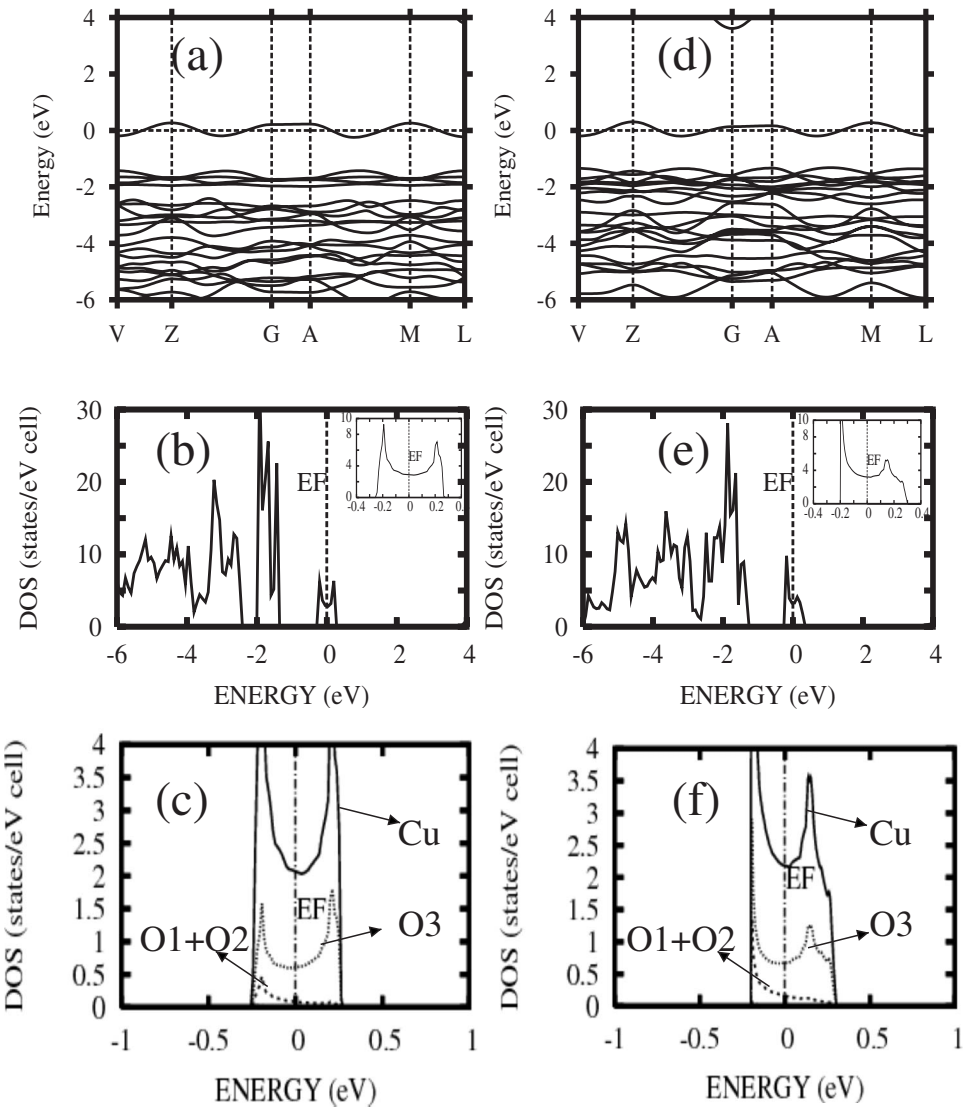

FIG. 2. Band structure, density of states, and partial DOS of [(a)–(c)] $Ba_2Cu(PO_4)_2$ and [(d)–(f)] $Sr_2Cu(PO_4)_2$.

of deriving a few-orbital effective Hamiltonian from the full LDA Hamiltonian by integrating out high-energy degrees of freedom.

III. RESULTS AND DISCUSSION

The all-orbital band structure and the total density of states (DOS) and partial DOS for $Ba_2Cu(PO_4)_2$ and $Sr_2Cu(PO_4)_2$ are displayed in Fig. 2. The bands are plotted along the various high symmetry points of the Brillouin zone corresponding to the monoclinic lattice. All the energies are measured with respect to the Fermi level of the compound. The characteristic feature of the non-spin-polarized band structure displayed in Figs. 2(a) and 2(d) is an isolated half-filled band at the Fermi level. This band is predominantly derived from the antibonding linear combination of Cu $d_{x^2-y^2}$ and O p_σ states residing in the same square plaquette. The conduction band is separated from the other Cu d character dominated valence bands by a small gap. This is consistent with the schematic energy level diagram displayed in Fig. 1(c). Further below these Cu d bands are the bands with predominantly oxygen $2p$ character. The conduction band disperses only along the chain direction with hardly any dispersion perpendicular to the chains. This is reflected in the partial DOS shown in the inset of Figs. 2(b) and 2(e), which has a characteristic feature of 1D tight-binding dispersion.

This isolated Cu $d_{x^2-y^2}$ conduction band is responsible for the low-energy physics of this material. This band hardly couples with any other states except for the oxygens (O3) residing in the square plaquette, as can be seen from the plot of the oxygen partial density of states displayed in Figs. 2(c) and 2(f). Since the calculations are carried out in the framework of LDA, the system is not insulating. We have checked that the insulating behavior can be recovered by including the Coulomb interaction in the framework of LDA+U. In the following, we shall employ NMTO downfolding method to map our LDA results to a low-energy orthogonal tight-binding Hamiltonian. This Hamiltonian will serve as the single electron part of the correlated Hubbard model relevant for this system, which, in turn, can be mapped to an extended Heisenberg model [Eq. (1)] with the exchange couplings related to the LDA hoppings by the relation

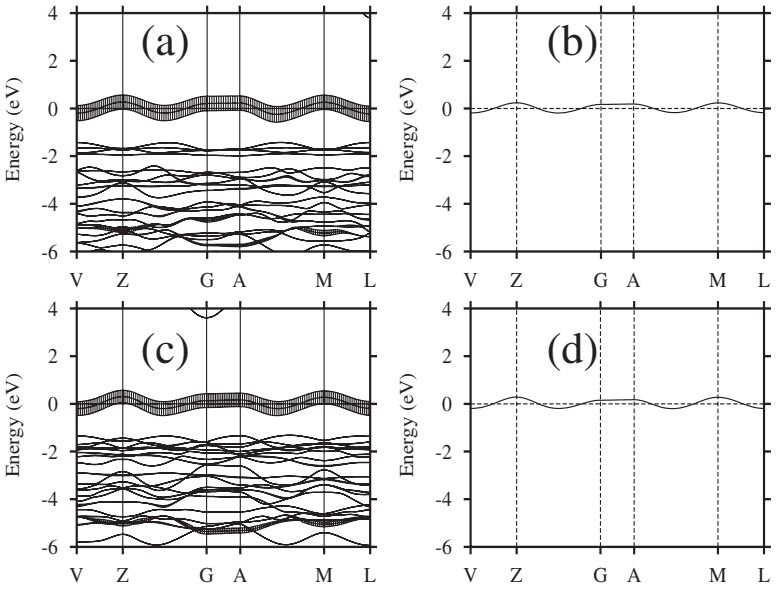

FIG. 3. Cu $d_{x^2-y^2}$ projected as well as downfolded band in [(a) and (b)] $Ba_2Cu(PO_4)_2$ and [(c) and (d)] $Sr_2Cu(PO_4)_2$.

$$J_{ij} = \frac{4t_{ij}^2}{U_{eff}}, \tag{2}$$

where U_{eff} is the screened Coulomb interaction.

The NMTO downfolding method provides an *ab initio* scheme to construct a low-energy tight-binding Hamiltonian starting from the full all-orbital LDA calculations. This method relies on the energy-selective downfolding process to integrate out high-energy degrees of freedom resulting in a low-energy Hamiltonian defined in the basis of effective orbitals. These effective orbitals, by construction, are tailored to contain in their tails the states which are integrated out with weights being proportional to their admixture with the orbitals that are retained in the basis. If the low-energy set of bands are separated from all other bands, the orthonormalized NMTO set converges to a set of Wannier functions. Hence, with the NMTO downfolding method, we can generate localized Wannier functions directly without recourse to Bloch functions. These effective orbitals (NMTOs) provide a direct visualization of the various interaction paths. The Fourier transform of this few-orbital downfolded Hamiltonian provides various hopping integrals t_{ij} between these effective orbitals, and the corresponding tight-binding Hamiltonian can be written as

$$H_{TB} = \sum_{(ij)} t_{ij}(c_i^\dagger c_j + \text{H.c.}), \tag{3}$$

where i and j denote a pair of orbitals. These hopping integrals thus form the first principles set of parameters obtained without any fitting procedure containing the signature of the pathways involved in the hopping process.

For the present compounds with one predominantly Cu $d_{x^2-y^2}$ band so well separated from the rest, one can have a tight-binding model with a single Cu $d_{x^2-y^2}$ orbital per Cu to be a good approximation to the full band structure close to the Fermi level. In Fig. 3, we have displayed the band structure of $Ba_2Cu(PO_4)_2$ and $Sr_2Cu(PO_4)_2$ decorated with Cu $d_{x^2-y^2}$ character together with the downfolded band structure where only Cu $d_{x^2-y^2}$ orbital is retained in the basis and the rest are downfolded. The agreement between the two is remarkable, suggesting that our one band Hamiltonian is indeed physically reasonable and is suitable to capture the low-energy physics of the system. The Fourier transform of the downfolded Hamiltonian $H(k) \rightarrow H(R)$ gives the effective hopping parameters for the physical Hamiltonian. In Table I, we have displayed the various dominant effective hopping integrals t_{ij} (having magnitude $\geqslant 1$ meV) between the Cu^{2+} ions at sites i and j. The notations for various hoppings for a pair of Cu sites (i and j) are indicated in Fig. 1(b), where, e.g., for a Cu ion at site i, $t_{ij}=t_1$ if the other Cu ion at site j is at the nearest neighbor-position along the chain and similarly for all the other hoppings.

From Table I, we gather that the nearest-neighbor hopping (t_1) is dominant for both the compounds. The other hoppings (t_2) along the chain (intrachain) as well as between the chains (interchain) (t_1^{ic}, t_2^{ic}) and between chains in the perpendicular (c) direction ($t_\perp$) are an order of magnitude smaller than the dominant nearest-neighbor hopping. The smaller magnitude of the hopping for $Ba_2Cu(PO_4)_2$ may be attributed to the relatively large lattice constant for the compound. Recently, these hoppings were also calculated by adopting a fitting procedure.[19] Although the trends among the hoppings obtained by fitting the conduction band agree with our *ab initio* results, the magnitude as well as the range of the hoppings are exaggerated in the fitting scheme.

In Fig. 4, we have displayed the Cu $d_{x^2-y^2}$ Wannier function. We note that for both the compounds, the Cu $d_{x^2-y^2}$

TABLE I. Hopping integrals obtained from our *ab initio* analysis for $Ba_2Cu(PO_4)_2$ and $Sr_2Cu(PO_4)_2$.

	t_1 (meV)	t_2 (meV)	t_1^{ic}	t_2^{ic}	$t_\perp$
$Ba_2Cu(PO_4)_2$	96	4	5	1	2
$Sr_2Cu(PO_4)_2$	103	9	14	0	1

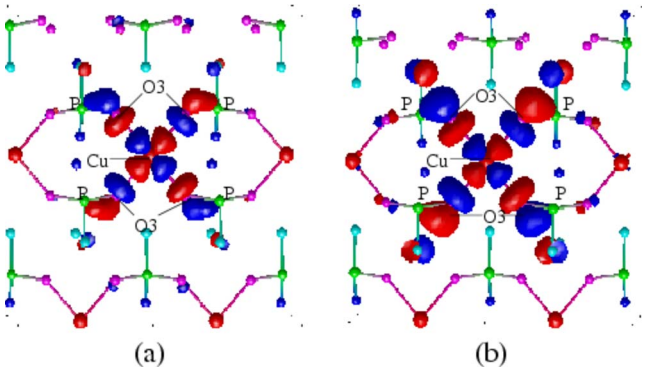

FIG. 4. (Color online) Effective Cu $d_{x^2-y^2}$ Wannier function plot for (a) $Ba_2Cu(PO_4)_2$ and (b) $Sr_2Cu(PO_4)_2$. The $d_{x^2-y^2}$ orbital is defined with the choice of local coordinate system as discussed in the text. The spheres represent the ions as indicated in the figure.

Wannier function is primarily localized in one plaquette and it hardly couples with the neighboring plaquettes. The tails of the Cu $d_{x^2-y^2}$ orbital are shaped according to O p_x/p_y orbitals such that the Cu $d_{x^2-y^2}$ orbital forms strong $pd\sigma$ antibonds with the O p_x/p_y tails. We also note that the Cu $d_{x^2-y^2}$ Wannier function for $Ba_2Cu(PO_4)_2$ is more localized, explaining the smaller magnitude of the hoppings for this system.

The hopping parameters listed in Table I can be used to estimate various exchange interactions using Eq. (2). In the absence of a satisfactory way of direct computation of exchange integrals, such an approximate method is a good starting point for estimating the exchange couplings as well as the relative strengths of the various exchange integrals. The ratios of the various exchange interactions for each compound are listed in Table II. As expected, the nearest-neighbor exchange interaction is dominant for both the compounds with practically negligible interchain and further-neighbor intrachain interactions, making these compounds ideal 1D HAFs spanning a wide temperature range. The agreement between the ratio of the nearest-neighbor exchange interaction in $Ba_2Cu(PO_4)_2$ to that in $Sr_2Cu(PO_4)_2$, $\frac{J_{Ba}}{J_{Sr}}$, obtained in our calculation and that obtained from experiment is remarkable. In the following, we shall try to understand the origin of the short-range hopping and therefore the exchange interactions in these systems. From the Cu $d_{x^2-y^2}$ Wannier function (Fig. 4), we gather that the Cu-Cu hopping primarily proceeds via the oxygens. As a result, as argued by Koo *et al.*[20] the strength of the Cu-O…Cu spin exchange is primarily governed by the O…O distance and Cu-O..Cu angles rather than the Cu..Cu distances. The exchange interaction therefore becomes negligible when the relative separation between the oxygens mediating the interaction is large compared to the van der Waals distance. For the present compounds, the weak hopping integrals and therefore the exchange interactions between the Cu ions may be attributed to their peculiar geometry. The CuO_4 plaquettes in the present compounds share neither edges nor corners and are connected by PO_4 tetrahedra resulting in a super-super exchange process to mediate the exchange interactions. This arrangement results in a large relative separation (greater than the van der Waals distance) between the oxygens except for the oxygens in the neighboring plaquettes along the chain, resulting in an appreciable nearest-neighbor interaction while other intrachain as well as interchain interactions are negligible.

TABLE II. Ratios of the exchange coupling constants and comparison with experiment for $Ba_2Cu(PO_4)_2$ and $Sr_2Cu(PO_4)_2$.

	J_2/J_1	J_{1ic}/J_1	J_{Ba}/J_{Sr}[a]	J_{Ba}/J_{Sr}[b]
$Ba_2Cu(PO_4)_2$	0.0017	0.0027	0.869	0.915
$Sr_2Cu(PO_4)_2$	0.0076	0.0184		

[a]Ratio of J/k_B of $Ba_2Cu(PO_4)_2$ to that of $Sr_2Cu(PO_4)_2$ obtained from theory.

[b]Ratio of J/k_B of $Ba_2Cu(PO_4)_2$ to that of $Sr_2Cu(PO_4)_2$ obtained from experiment (Ref. 10).

As mentioned earlier, even tiny interchain interactions can cause a deviation from the ideal 1D behavior. Indeed, in the ^{31}P NMR shift (which is proportional to the spin susceptibility) measurements on $Ba_2Cu(PO_4)_2$ and $Sr_2Cu(PO_4)_2$,[10] it was found that while the data are well described by the 1D HAF model in a large temperature range, a sharp deviation was seen below $k_BT/J \approx 0.03$ (still above the LRO temperature found by Belik *et al.*[9]). A small interchain interaction can therefore be of significance at very low temperatures. In order to check that small interchain hoppings are indeed important, we calculated the zero-temperature spin-spin correlation function for a pair of staggered $S=\frac{1}{2}$ Heisenberg chains [see Fig. 1(b)] (24 sites, with periodic boundary conditions) using the exact diagonalization method. We confirmed that in the absence of interchain coupling, the spin-spin correlation function decays with a characteristic power-law behavior. However, inclusion of a very tiny interchain coupling $\frac{J_{ic}}{J_1} \approx 0.02$ causes the spin-spin correlation function to deviate from the power-law behavior and acquire an exponential decay. This might then be responsible for the sharp decrease in the ^{31}P NMR shift seen at low-temperatures by Nath *et al.*[10]

IV. SUMMARY AND CONCLUSIONS

We have employed TB-LMTO ASA and NMTO method to analyze in detail the electronic structure of two isostructural phosphates, $Ba_2Cu(PO_4)_2$ and $Sr_2Cu(PO_4)_2$. The characteristic feature of the LDA electronic structure of these compounds is an isolated half-filled band at the Fermi level derived from the antibonding linear combination of Cu $d_{x^2-y^2}$ and oxygen p_σ states residing on CuO_4 square plaquettes. The various hopping integrals obtained using NMTO downfolding method suggest that these compounds are indeed one dimensional with dominant nearest-neighbor hopping integrals along the chains. Our estimate of the exchange interaction, in particular, the ratio of the exchange interaction of $Sr_2Cu(PO_4)_2$ to that of $Ba_2Cu(PO_4)_2$, compares excellently with the experimental results. The plot of the Cu $d_{x^2-y^2}$ Wannier functions suggests that the exchange interactions between the magnetic Cu^{2+} ions are primarily mediated by the oxygens. Our calculations confirm that the unique geometry of the CuO_4 plaquettes, which are neither face sharing nor

corner sharing, is responsible for the unique 1D magnetic properties for these systems. Finally, we argue that although the interchain couplings are small, they may still be important for the low-temperature properties for this system and may explain the sharp deviation from the 1D HAF model at low temperature seen in the ^{31}P NMR shift for these systems.

ACKNOWLEDGMENTS

I.D. thanks the DST, India (Project No. SR/S2/CMP-19/2004) for financial support. A.V.M. thanks the Alexander von Humboldt Foundation for the financial support for the stay at Augsburg.

*Present address: Jamia Millia Islamia, New Delhi-110025, India.
†Present address: Max-Planck-Institute for Chemical Physics of Solids, Nöthnitzer Strasse 40, 01187 Dresden, Germany.
‡dasgupta@phy.iitb.ac.in

[1] P. Lemmens, G. Güntherodt, and C. Gros, Phys. Rep. **375**, 1 (2003).
[2] C. K. Majumdar and D. K. Ghosh, J. Math. Phys. **10**, 1388 (1969).
[3] F. D. M. Haldane, Phys. Rev. Lett. **60**, 635 (1988).
[4] E. Dagotto and T. Rice, Science **271**, 618 (1996).
[5] M. Hase, I. Terasaki, and K. Uchinokura, Phys. Rev. Lett. **70**, 3651 (1993).
[6] E. Dagotto, Rep. Prog. Phys. **62**, 1525 (1999).
[7] M. Azuma, Z. Hiroi, M. Takano, K. Ishida, and Y. Kitaoka, Phys. Rev. Lett. **73**, 3463 (1994).
[8] T. Asano, H. Nojiri, W. Higemoto, A. Koda, R. Kadono, and Y. Ajiro, J. Phys. Soc. Jpn. **71**, 594 (2002).
[9] A. A. Belik, S. Uji, T. Terashima, and E. Takayama-Muromachi, J. Solid State Chem. **178**, 3461 (2005).
[10] R. Nath, A. V. Mahajan, N. Buttgen, C. Kegler, A. Loidl, and J. Bobroff, Phys. Rev. B **71**, 174436 (2005).
[11] D. C. Johnston, R. K. Kremer, M. Troyer, X. Wang, A. Klumper, S. L. Budko, A. F. Panchula, and P. C. Canfield, Phys. Rev. B **61**, 9558 (2000).
[12] A. A. Belik, M. Azuma, and M. Takano, J. Solid State Chem. **177**, 883 (2004).
[13] O. K. Andersen and O. Jepsen, Phys. Rev. Lett. **53**, 2571 (1984).
[14] O. Jepsen and O. K. Andersen, STUTTGART TB-LMTO program, Version 47, 2000.
[15] O. Jepsen and O. K. Andersen, Solid State Commun. **9**, 1763 (1971).
[16] O. K. Andersen and T. Saha-Dasgupta, Phys. Rev. B **62**, R16219 (2000).
[17] O. K. Andersen, T. Saha-Dasgupta, R. W. Tank, C. Arcangeli, O. Jepsen, and G. Krier, *Electronic Structure and Physical Properties of Solids: The Uses of the LMTO Method*, Springer Lecture Notes in Physics Vol. 535 (Springer, New York, 2000), pp. 3–84.
[18] O. K. Andersen, T. Saha-Dasgupta, and S. Ezhov, Bull. Mater. Sci. **26**, 19 (2003).
[19] M. D. Johannes, J. Richter, S.-L. Drechsler, and H. Rosner, Phys. Rev. B **74**, 174435 (2006).
[20] H.-J. Koo, D. Dai, and M.-H. Whangbo, Inorg. Chem. **44**, 4359 (2005).